Spontaneous dissociation and rovibrational structure of the metastable D_2^- anion

Ferid Mezdari,[1,*] Nathalie de Ruette,[2] and Xavier Urbain[3]
[1]*Department of Physics, Faculty of Sciences, University of Gabès, 6029 Gabès, Tunisia*
[2]*Department of Physics, Stockholm University, SE-106 91 Stockholm, Sweden*
[3]*Institute of Condensed Matter and Nanosciences, Université catholique de Louvain, B-1348 Louvain-la-Neuve, Belgium*
(Received 17 August 2017; published 29 September 2017)

Long-lived rovibrational states of the metastable D_2^- molecular anion, with lifetimes of the order of microseconds, were studied by recording the time-of-flight difference between D and D^- fragments produced by spontaneous dissociation of the D_2^- complex. The simulated time-of-flight spectrum was adjusted to the experimental results, allowing us to extract the resonance energy relative to the dissociation threshold. A single value was found, 22.8 ± 0.3 meV, which is somewhat larger than resonance energies predicted by theory for long-lived D_2^- rovibrational states with (J,v) quantum numbers (37,0), (37,1), and (38,0) [Phys. Rev. A **75**, 012507 (2007)]. This discrepancy seems due to the extreme sensitivity of these metastable states to minute features of the potential energy curve. The spectral feature is explained by the competition between autodetachment and spontaneous dissociation decay channels.

DOI: 10.1103/PhysRevA.96.032512

I. INTRODUCTION

The molecular hydrogen anion is of major theoretical interest as a benchmark to develop models and basis sets for highly correlated, few electron systems. This fundamental negative ion, considered as a collisional system, contributes to the ion chemistry of many astrophysical environments and controlled thermonuclear fusion plasmas.

Electron-induced vibrational excitation of H_2, and dissociative electron attachment, i.e., $H_2 + e^- \rightarrow H + H^-$, are mediated by the resonant electron capture to the ground $X\ ^2\Sigma_u^+$ and excited $A\ ^2\Sigma_g^+$ states of H_2^- [1]. The large autodetachment width of those resonances embedded in the electronic continuum, together with the unfavorable Franck-Condon overlap, are responsible for the extreme vibrational and isotopic sensitivity of dissociative attachment [2,3].

The reverse process, associative detachment, i.e., $H + H^- \rightarrow H_2 + e^-$, was recognized as a key formation mechanism of ground state molecular hydrogen in the early Universe [4]. The actual shape of the cross section versus collision energy reflects the details of the H_2^- potential energy curve, in particular the presence of a short-range barrier, and the growing influence of the long-range centrifugal barrier with increasing collision energy [2,5].

The existence, structure, and lifetime of the molecular hydrogen anions was, for a long time, a matter of debate, both experimentally and theoretically. Since 1975, mass-spectrometric observations claim the existence of H_2^-, D_2^- and HD^- with lifetimes greater than 10^{-5} s [6], although mass-spectrometric detection of H_2^- was already reported in 1958 [7], and again in 1974 [8]. Later on, Bae *et al.* [9] concluded, after an unsuccessful attempt to produce H_2^- by a two-step electron capture technique, to the nonexistence of the metastable H_2^- complex. After several years of continued experimental effort, the existence of long-lived molecular hydrogen anions was definitely established [10,11] by accelerator mass spectrometry.

These anionic species are produced either by sputtering TiH_2 and TiD_2 with Cs^+, or in a discharge ion source. To increase the production yield of H_2^- in a high-voltage corona-discharge source coupled to a supersonic jet, Rudnev *et al.* [12] used acetylene gas mixed in N_2 and CO_2 instead of pure hydrogen. Whether the mode of production affects the population of the rovibrational levels of H_2^- is still to be investigated.

Lifetimes have been measured for all of three isotopologues H_2^-, D_2^-, and HD^-, using an electrostatic ion-beam trap [13]. The measured lifetimes of H_2^- and HD^- were 8.2 and 50.7 μs, respectively. For D_2^-, three decay time constants were measured, i.e., 23, 84, and 1890 μs. Rovibrational states of H_2^- and D_2^- were also studied in coincidence photofragmentation experiments [14], as well as in foil-induced Coulomb explosion imaging measurements [15,16]. The photodetachment cross section of the H_2^- anion was measured by beam depletion in a narrow wavelength range [12]. An unexpected oscillatory behavior of the depletion cross section was observed, which was tentatively ascribed to the rotating dipole of the fast-spinning molecule.

Theoretical calculations [2,17–19] for the description of the nuclear dynamics of H_2^- collision complex and its isotopic analogues, D_2^-, HD^-, and T_2^- were performed within a nonlocal resonance model. The resonances in the $X\ ^2\Sigma_u^+$ electronic state of H_2^- are stabilized against autodetachment by molecular rotation at high angular momenta [19], causing the potential energy minimum of the H_2^- ground state to lie outside of the potential well of H_2 (see Fig. 7). The metastability of these molecular complexes against dissociation is assigned [10] to the existence of a wide centrifugal barrier. Cízek and Horácek [19] computed the lifetimes and resonance energies relative to the dissociation threshold of several rovibrational states of H_2^-, D_2^-, HD^-, and T_2^- molecular complexes. The lifetimes and corresponding energy levels obtained for D_2^- are 61, 16, and 2108 μs and 2, 18, and 19 meV, for $(J,v) = (37,0)$, (37,1), and (38,0) rovibrational states, respectively. These strongly differ from those obtained earlier by R. Golser *et al.* [10], i.e., 14 and 7.2 μs, for the (37,0) and (38,0) states, respectively.

*feridmez@yahoo.fr

There clearly remain some discrepancies between various authors that require more investigations both on the experimental and theoretical side. To further unravel the structure of the molecular hydrogen anion D_2^-, and shed light on the lifetimes and energies of rovibrational states that are long-lived enough to be observed on the time scale of our experiment ($\sim 5\ \mu$s), we measured the kinetic energy released by spontaneous dissociation of the D_2^- complex. This decay channel that was so far overlooked in experimental studies, offers a stringent test of the state energies and lifetimes as calculated by M. Cízek and Horácek [19].

This paper is organized as follows: In Sec. II we describe our experimental setup, in Sec. III we present the experimental results and Monte Carlo simulations of the time-of-flight distribution, in Sec. IV results are discussed and compared to theoretical results, and we summarize our findings in Sec. V.

II. EXPERIMENTAL SETUP

The merged beam apparatus used in the present study has been described elsewhere [20–23]. The sections of this apparatus are displayed schematically in Fig. 1. The acceleration is provided by one branch of our merged beam setup. The beam is extracted from a duoplasmatron source fed with deuterium gas. The beam travels 1.6 m successively through a Wien filter for mass selection, and deflectors and collimators aimed at clearing the beam from particles generated by spontaneous decay along the flight path. The ion beam is monitored by means of retractable probes. The beam enters the observation cell evacuated to ultrahigh vacuum ($\sim 10^{-10}$ mbar) and consisting of a set of parallel metal plates perpendicular to the beam axis, each plate having a circular hole centered on that axis (see Fig. 1). An electrical potential $U_{\rm obs}$ is applied on these plates. This bias voltage serves as a tag for the pairs of particles formed in the observation cell to be detected in coincidence.

In the present configuration, the observation cell is followed by a pair of vertical and horizontal deflectors and a long flight tube appropriately screened against Earth's magnetic field by μ-metal shielding. A pair of position-sensitive detectors consisting of a Z stack of multichannel plates and a resistive anode are located at the end of the beam line, 2.725 and 2.825 m from the center of the observation chamber, respectively. The detectors (40 mm diameter active area) are displaced longitudinally to minimize the transverse gap between them. The time and position of the impacts are recorded by a dedicated multiplexer reading the outputs of the position

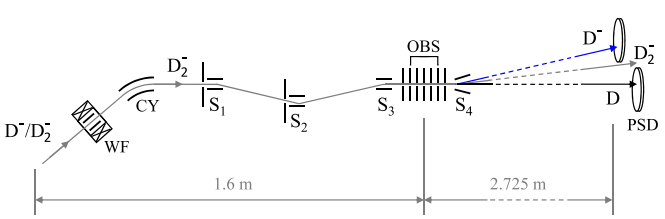

FIG. 1. Schematic diagram of the experimental setup (not to scale). WF, Wien filter; CY, cylindrical deflector; S1 to S4, electrostatic steerers; OBS, biased observation cell; PSD, position sensitive detectors.

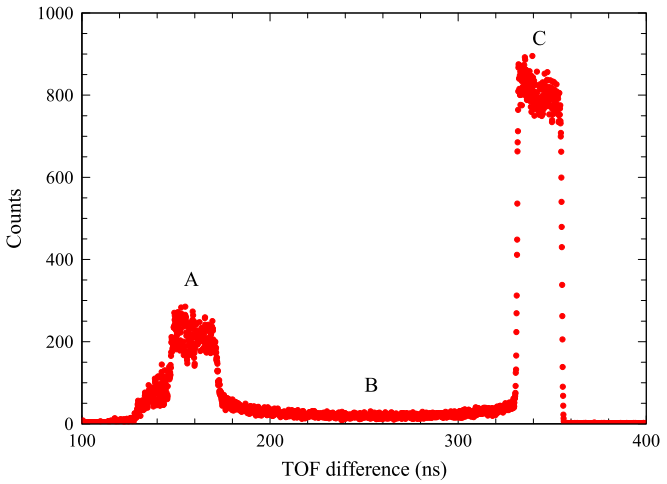

FIG. 2. Experimental time-of-flight difference between D and D^- fragments for a beam energy $E_b = 10$ keV, and a bias voltage $U_{\rm obs} = -500$ V. Three contributions may be identified. (A) dissociations occurring before and after the observation cell, (B) dissociations occurring in the voltage gradients, (C) dissociations occurring inside the observation cell.

encoders and the combination of a time-to-amplitude and an analog-to-digital converter. Due to the long time-of-flight to be measured with high accuracy, a double time reference is recorded for each actual coincidence event, with respective delay 0 and 500 ns, the latter from a digital gate and delay generator (Stanford Research Systems). This allows us to compensate for long-term drifts of the timing electronics.

With both deflectors off at the exit of the observation cell, an attenuated D_2^- beam is first aimed at the back detector. A voltage is then applied to steer the beam in the dead area between the detectors before restoring the full beam intensity ($\sim$0.1 pA). With this setting, neutral fragments are expected to hit the back detector while D^- fragments, carrying half the kinetic energy of the parent beam, will experience a stronger deflection and end up on the front detector. This deflection does not affect their time-of-flight, while the action of the observation voltage is to accelerate D^- with respect to D, thereby discriminating events occurring inside the observation cell from those happening elsewhere. This selection is illustrated in Fig. 2, where tagged events accumulate in peak C due to the acceleration of D^- with respect to D, hence the corresponding increase of the time separation between them. Three-dimensional imaging of the dissociation is only possible if the actual D^- trajectory is known with sufficient precision, which is intractable here due to stray electric and magnetic fields affecting the ions along their flight. Nevertheless, the sole time-of-flight difference suffices to retrieve the kinetic energy released by spontaneous dissociation in the observation cell, as demonstrated in the next section.

III. KINETIC ENERGY RELEASE DETERMINATION

The time-of-flight of D and D^- produced by spontaneous dissociation of the D_2^- parent anion at various locations of the above-described apparatus, were simulated with the goal

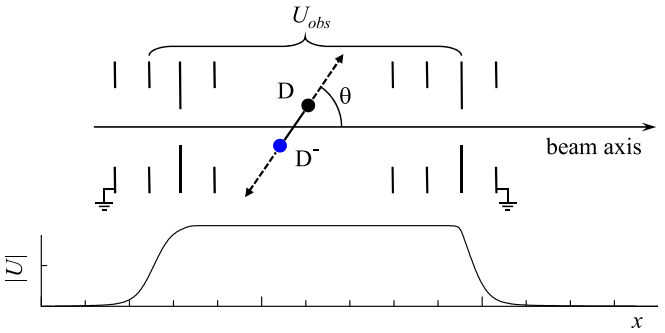

FIG. 3. Schematic illustration of the D_2^- dissociation in the observation cell (not to scale). Also displayed is the actual profile of the electrical potential along the beam axis, to be scaled by the value of U_{obs} (e.g., −500 V for 10 keV).

to retrieve the kinetic energy released by the dissociation. For this purpose, we computed the electrostatic potential along the axis of the observation cell (Fig. 3). These calculations were performed with a 0.1 mm step, over a distance $d = 141$ mm separating steerers S_3 and S_4 (see Fig. 1), between which the observation cell is located. This potential will affect the dissociations taking place within a small area around the center of the observation chamber, since both the parent anion and its charged fragment will decelerate or accelerate in the potential gradients.

Following the Monte Carlo approach, the x position of the dissociation is randomly chosen between the entrance and the exit of the observation cell, and the D_2^- anion is randomly oriented in space, as depicted in Fig. 3. The x component of the velocities of D and D^- along the beam axis at the dissociation position is given by

$$v_x = \sqrt{\frac{E_b - qU(x)}{m_D}} \pm \frac{1}{2}\cos\theta\sqrt{\frac{2E_{kin}}{\mu}}, \qquad (1)$$

where E_b is the D_2^- beam energy, $U(x)$ is the electrostatic potential at dissociation position x, E_{kin} is the kinetic energy released in the fragmentation of D_2^- molecular ion, m_D is the atomic deuterium mass, and $\mu = m_D/2$ denotes the reduced mass of D_2^- system.

Unlike the neutral species D, the D^- ion velocity will continue to vary after dissociation, as a result of the electrostatic potential applied to the parallel plates of the observation cell. We have taken this effect into account in our calculations. Since we know the distance between the center of the observation chamber and the detectors (2.825 m for the D fragment and 2.725 m for the D^- fragment), we computed the time-of-flight difference between the two fragments (see Fig. 4). In these calculations, two parameters were optimized, the kinetic-energy release E_{kin} and the number of events. A chi-square test χ^2 for goodness of fit of the experimental spectrum of time-of-flight differences was performed (Fig. 5). We calculated the χ^2 distribution for different values of the kinetic energy release E_{kin} with 0.1 meV resolution. The best kinetic energy release parameter E_{kin} corresponds to the minimum of the χ^2 distribution. Since E_{kin} is identified as the position of an energy level, it gives access to the rovibrational structure of the metastable D_2^- anion, as discussed below.

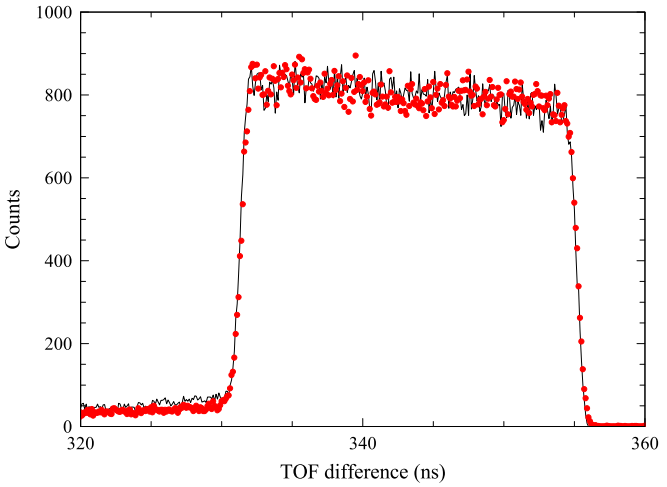

FIG. 4. Experimental (full circles) and simulated (full line) time-of-flight difference between D and D^- fragments for beam energy $E_b = 10$ keV, bias voltage $U_{obs} = -500$ V, and kinetic energy release $E_{kin} = 22.8$ meV, as obtained from the best fit.

IV. RESULTS AND DISCUSSION

The time-of-flight difference spectrum was measured for beam energies equal to 3, 6, and 10 keV. These beam energies correspond to time-of-flight from the ion source into the observation cell t_{obs} equal to 4.4, 3.1, and 2.4 μs, respectively. For all three cases, this spectrum was simulated, and the value of the kinetic energy release E_{kin} was fitted to the experimental data. Figure 4 displays our measured time-of-flight difference spectrum for a beam energy of 10 keV, and the calculated one, with a kinetic energy release parameter $E_{kin} = 22.8$ meV. We see a good agreement between measured and calculated spectra. A χ^2 calculation has been used to test the goodness of the fit between the experimental spectrum and the calculated one, for different values of the E_{kin} parameter. The χ^2 distribution is shown in Fig. 5 for a beam energy of 10 keV. The

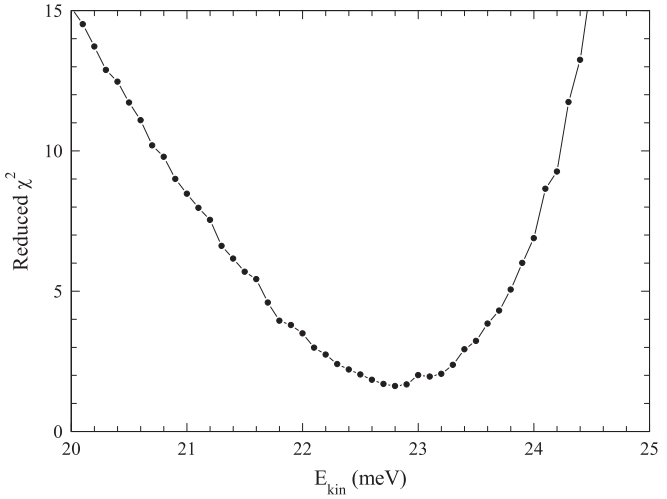

FIG. 5. Reduced χ^2 distribution obtained for different values of the kinetic energy release, used in the Monte Carlo simulation of the time-of-flight difference spectrum of the fragmentation of D_2^-.

TABLE I. Time-of-flight from the source to the observation cell, t_{obs}, and measured kinetic energy release, E_{kin} as a function of beam energy, for the spontaneous dissociation of D_2^-.

Beam energy (keV)	t_{obs} (μs)	E_{kin} (meV)
3	4.4	22.9 ± 0.9
6	3.1	22.9 ± 0.6
10	2.4	22.8 ± 0.4
Weighted mean		22.8 ± 0.3

E_{kin} best-fit value and its uncertainty are obtained by Taylor series expansion of χ^2 around its minimum. The obtained kinetic energy releases are identical in all three cases within the error bar (see Table I). The weighted mean of these three values is 22.8 ± 0.3 meV.

According to theoretical predictions [19], three states should be long-lived enough to be observed on the time scale of our experiment ($\sim$5 μs). These states are the (37,0), (37,1), and (38,0) rovibrational states with respective decay constant 61, 16, and 2108 μs, and the corresponding resonance energies relative to the dissociation threshold are 2, 18, and 19 meV, respectively [10,19]. However, a single contribution appears in our time-of-flight spectrum, for which an E_{kin} value equal to 22.8 ± 0.3 meV was obtained, which most likely corresponds to a single rovibrational state.

To unravel this discrepancy between theory and experiment, we have calculated the time-of-flight spectrum with the theoretical parameters given by Ref. [19]. These parameters are displayed in Table II. The fractional contribution P_i of each state to the spontaneous dissociation spectrum is given by

$$P_i = \frac{f_i/\tau_i}{\sum_k f_k/\tau_k}, \tag{2}$$

where τ_i is the theoretical lifetime, and f_i the population of each state in the beam within our observation cell. The latter populations are obtained by first correcting the populations f_i^H measured by Herwig *et al.* [16] for their decay during the time-of-flight from the ion source in that experiment ($t_H \sim 10$ μs), then taking into account the exponential decay to our observation cell:

$$f_i = f_i^H \exp\left[(t_H - t_{obs})/\tau_i\right]. \tag{3}$$

TABLE II. Input parameters used in the simulation of the time-of-flight spectrum shown in Fig. 6. Quantum numbers J and v are given for each state. τ_i is the predicted lifetime of state i [19], f_i its population in the beam within our observation cell (obtained from the results of [16]), P_i its fractional contribution to the decay signal over the length of the observation cell, and E_i is the theoretical resonance energy relative to the dissociation threshold [10,19].

J	v	τ_i (μs)	f_i	P_i	E_i (meV)
37	0	61	24	0.101	2
37	1	16	47	0.895	18
38	0	2108	29	0.004	19

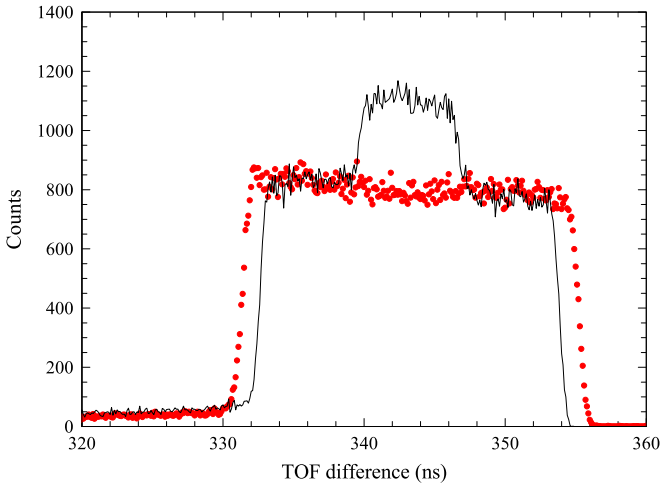

FIG. 6. Experimental (full circles) and simulated (full line) time-of-flight difference of D and D^- fragments for a beam energy of 10 keV. Calculations are done with three weighted contributions corresponding to kinetic energies E_{kin} equal to 2, 18, and 19 meV, under the assumption that all resonances decay by tunneling through the centrifugal barrier.

The expected spectrum, as calculated with the parameters above (see Table II), is shown in Fig. 6. In this calculation, the contribution of all three rovibrational states (37,0), (37,1), and (38,0) is taken into account; each resonance energy E_i relative to the dissociation threshold is weighted by its fractional contribution P_i. In this figure, we can see the structures (two levels) that correspond to the (37,0) state (upper level) and the (37,1) state (lower level). The contribution of the third state (38,0) is too small to be noticeable (0.4 % see Table II). In this model we assume that spontaneous dissociation, i.e., $D_2^- \rightarrow D + D^-$, is the dominant decay channel. An identical time-of-flight spectrum would have been obtained if all levels had the same dissociation branching ratio.

Some hypotheses may be formulated to account for the difference between the measured spectrum and the expected one. The first hypothesis is that only one state is long-lived enough to be observed on the time scale of our experiment ($\sim$5 μs). But, this hypothesis is in disagreement with the three decay constants observed in the experiment of Heber *et al.* [13]. As a second possibility, it may well be that the resonance energies of the above-mentioned states are quite similar, so that we cannot resolve them in our experiment. However, our experimental resolution is better than 1 meV, sufficient to resolve the three resonance energies given by Cízek and Horácek [19] for the (37,0), (37,1), and (38,0) rovibrational states, provided that they individually contribute to the recorded spectrum.

A third hypothesis rests on the existence of a large potential barrier for the (37,0) state (see Fig. 7 and potential-energy curves in Refs. [2,14]). The only decay channel permitted for this state is the autodetachment by quantum tunneling, i.e., $D_2^- \rightarrow D_2 + e^-$. Note that we are not able to detect the autodetachment channel with our setup, as we rely on coincident detection. Consequently, no or very little contribution of the (37,0) state to the dissociation will appear on the measured time-of-flight spectrum. For the (37,1) state the two decay

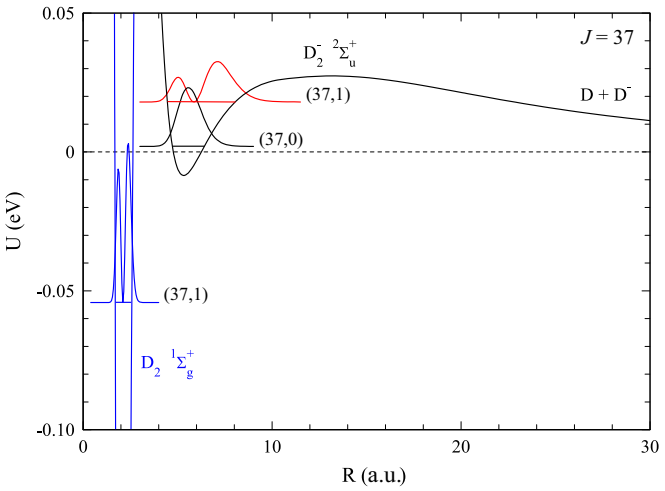

FIG. 7. Potential energy diagram for D_2 and D_2^- at $J = 37$. Also shown are the radial probability densities $|\psi(R)|^2$ for $D_2(37,1)$ (in blue), $D_2^-(37,0)$ (in black), and $D_2^-(37,1)$ (in red).

channels, autodetachment and dissociation, are allowed by quantum tunneling, with unknown branching fraction. Finally, for the (38,0) state the lifetime $\tau = 2108$ μs (see Table II) [19] is much longer than the time-of-flight through the observation cell ($\sim$0.4 μs for the slowest D_2^- beam used). Therefore, this last state will have an undetectable contribution to the time-of-flight spectrum. We may thus conclude from the above discussion that a single state is efficiently contributing to the measured time-of-flight spectrum, as observed.

Let us now assume that the autodetachment decay rate Γ_{AD} of the (37,0) state is approximately equal to the autodetachment decay rate of the (37,1) state. For the (37,0) state, the dissociation decay rate $\Gamma_D \approx 0$ (see discussion above). Therefore, the lifetimes τ_0 and τ_1 of the (37,0) and (37,1) states are approximately given by

$$\tau_0 = 1/\Gamma_{AD}, \tag{4}$$

$$\tau_1 = 1/(\Gamma_{AD} + \Gamma_D). \tag{5}$$

The values of τ_0 and τ_1 are listed in Table II. Under these assumptions, we obtain the branching fraction of the (37,1) state toward autodetachment, f_{AD}, and toward dissociation, f_D, by rearranging Eqs. (4) and (5) as follows:

$$f_{AD} = \Gamma_{AD}/(\Gamma_{AD} + \Gamma_D) = \tau_1/\tau_0 = 0.26, \tag{6}$$

$$f_D = \Gamma_D/(\Gamma_{AD} + \Gamma_D) = 0.74. \tag{7}$$

The dissociation process appears to be the dominant decay mode for this state, but calculations or measurements of the respective decay rates are needed to confirm this tentative result.

The latter hypothesis is supported by existing theoretical studies [10,19], which predict that the centrifugal potential barrier of high angular momentum states combined with the pure electronic potential leads to a potential well at large internuclear distance R. This potential well reduces the decay by autodetachment, i.e., $D_2^- \rightarrow D_2 + e^-$, due to the poor overlap of the vibrational wave function of the D_2^- anion with those supported by the $X\ ^1\Sigma_g^+$ potential of the D_2 neutral system. Autodetachment was, however, observed to be a major decay channel for the H_2^- complex [15], which is more likely to tunnel due to smaller nuclear mass. On the other hand, to reach larger R, D_2^- has to tunnel through a low but wide potential barrier, which reduces the relaxation via the energetically allowed dissociation channel, i.e., $D_2^- \rightarrow D + D^-$.

The dissociation channel was observed in the measured time-of-flight spectrum with a resonance energy $E_{kin} = 22.8 \pm 0.3$ meV relative to the dissociation threshold, somewhat larger than the predicted resonance energy $E_{(37,1)} = 18$ meV [2,10]. Cízek *et al.* have tested the sensitivity of the resonance positions and lifetimes with respect to small changes in the effective interatomic potential. The resonances were found to shift by 3–7 meV with a slight modification of the outer well. In that respect, substantial differences exist between the potential energy curve for the H_2^- complex calculated by Cízek *et al.* [2] and those calculated by Srivastava *et al.* [24]. We therefore think that these resonance energies should be revised by further refining the calculation of the potential energy curve.

In addition, the proper assignment of these metastable D_2^- levels to specific (J,v) combinations was challenged by the coincidence experiment of Lammich *et al.* [14]. However, Herwig *et al.* [16] concluded in a more recent study that the original assignment was indeed valid. So, more effort, on both experimental and theoretical sides, should be deployed to clarify these discrepancies.

Finally, in a separate experiment, the D_2^- beam was aimed in the space between the detectors, and a large voltage applied to the last deflector prevented any ion from reaching them. No coincidence between neutral fragments was observed, indicating that the dissociative detachment decay channel $D_2^- \rightarrow D + D + e^-$ does not contribute to the decay process. This result agrees with earlier experimental findings by Bae *et al.* [9], who concluded to the inexistence of electronically excited H_2^-.

V. CONCLUSION

The spontaneous dissociation of the metastable D_2^- molecular anion was studied by measuring the corresponding time-of-flight spectrum. The time scale of our experiment corresponds to D_2^- states with lifetimes of the order of microseconds. Reproducing the measured spectrum by Monte Carlo simulation allowed us to extract the kinetic energy release (E_{kin}) identified as the resonance position relative to the D + D^- dissociation threshold. A single value was found, 22.8 ± 0.3 meV, which is somewhat larger than the theoretical resonance energies [10,19] predicted for long-lived D_2^- rovibrational states with (J,v) quantum numbers (37,0), (37,1), and (38,0). This discrepancy seems due to the extreme sensitivity of these metastable states to minute features of the potential-energy curves.

The observation of a single contribution was explained by the vanishing tunneling probability of the (37,0) state through the wide centrifugal barrier, contrary to the (37,1) state, which lies higher in the potential well. The branching fraction of the (37,1) state toward dissociation was predicted to be dominant under the assumption of identical autodetachment rate for the (37,0) and (37,1) states. The absence of the (38,0) contribution stems from its much longer lifetime.

From the absence of dissociative detachment, which would have produced pairs of D atoms, we conclude that the metastable D_2^- anion has a large internuclear equilibrium distance keeping the radial probability distribution outside the autodetachment region. This confirms the prediction of Cízek *et al.* [19] and earlier experimental observations [14–16].

In the light of this discussion, it seems that more effort, on both experimental and theoretical sides, should be deployed to confirm these findings. In particular, the branching fraction toward autodetachment versus spontaneous dissociation should be computed for all long-lived resonances, and their energies refined by improving the potential energy curve of the H_2^- system.

On the experimental side, the present approach may be extended to longer lifetimes by introducing an adjustable delay between the production of D_2^- and the observation of its spontaneous dissociation, by means of an electrostatic ion beam trap [25]. The measurement of electron spectra associated with autodetachment, as attempted by Rudnev *et al.* [12], should provide further insight into the rovibrational structure of these resonant states. An experimental characterization of these states definitely constitutes a benchmark for the theory of the small, highly correlated complexes.

ACKNOWLEDGMENTS

The authors thank C. Lauzin for fruitful discussions and M. Cízek for having provided the potential energy curve in numerical form. This work was supported by the Fonds de la Recherche Scientifique-FNRS through IISN Contract No. 4.4504.10. The authors thank the Belgian State for the grant allocated by Royal Decree for research in the domain of controlled thermonuclear fusion. N.dR. acknowledges a FRIA grant of the Fonds de la Recherche Scientifique-FNRS. F.M. thanks the Université catholique de Louvain for support, and the staff of the Institute of Condensed Matter and Nanosciences for the friendly environment and for help.

[1] G. J. Schulz and R. K. Asundi, Phys. Rev. Lett. **15**, 946 (1965).
[2] M. Cízek, J. Horácek, and W. Domcke, J. Phys. B **31**, 2571 (1998).
[3] E. Krishnakumar, S. Denifl, I. Cadez, S. Markelj, and N. J. Mason, Phys. Rev. Lett. **106**, 243201 (2011).
[4] H. Kreckel, H. Bruhns, M. Cízek, S. C. O. Glover, K. A. Miller, X. Urbain, and D. W. Savin, Science **329**, 69 (2010).
[5] K. A. Miller, H. Bruhns, J. Eliásek, M. Cízek, H. Kreckel, X. Urbain, and D. W. Savin, Phys. Rev. A **84**, 052709 (2011).
[6] W. Aberth, R. Schnitzer, and M. Anbar, Phys. Rev. Lett. **34**, 1600 (1975).
[7] V. I. Khvostenko and V. M. Dukel'skii, Sov. Phys. JETP **7**, 709 (1958).
[8] R. Hurley, Nucl. Instrum. Methods **118**, 307 (1974).
[9] Y. K. Bae, M. J. Coggiola, and J. R. Peterson, Phys. Rev. A **29**, 2888 (1984).
[10] R. Golser, H. Gnaser, W. Kutschera, A. Priller, P. Steier, A. Wallner, M. Cízek, J. Horácek, and W. Domcke, Phys. Rev. Lett. **94**, 223003 (2005).
[11] H. Gnaser and R. Golser, Phys. Rev. A **73**, 021202 (2006).
[12] V. Rudnev, M. Schlösser, H. H. Telle, and Á. G. Ureña, Chem. Phys. Lett. **639**, 41 (2015).
[13] O. Heber, R. Golser, H. Gnaser, D. Berkovits, Y. Toker, M. Eritt, M. L. Rappaport, and D. Zajfman, Phys. Rev. A **73**, 060501 (2006).
[14] L. Lammich, L. H. Andersen, G. Aravind, and H. B. Pedersen, Phys. Rev. A **80**, 023413 (2009).
[15] B. Jordon-Thaden, H. Kreckel, R. Golser, D. Schwalm, M. H. Berg, H. Buhr, H. Gnaser, M. Grieser, O. Heber, M. Lange, O. Novotný, S. Novotny, H. B. Pedersen, A. Petrignani, R. Repnow, H. Rubinstein, D. Shafir, A. Wolf, and D. Zajfman, Phys. Rev. Lett. **107**, 193003 (2011).
[16] P. Herwig, D. Schwalm, M. Cízek, R. Golser, M. Grieser, O. Heber, R. Repnow, A. Wolf, and H. Kreckel, Phys. Rev. A **87**, 062513 (2013).
[17] J. Horácek, M. Cízek, K. Houfek, P. Kolorenc, and W. Domcke, Phys. Rev. A **70**, 052712 (2004).
[18] J. Horácek, M. Cízek, K. Houfek, P. Kolorenc, and W. Domcke, Phys. Rev. A **73**, 022701 (2006).
[19] M. Cízek, J. Horácek, and W. Domcke, Phys. Rev. A **75**, 012507 (2007).
[20] S. Szücs, M. Karemera, M. Terao, and F. Brouillard, J. Phys. B **17**, 1613 (1984).
[21] K. Olamba, S. Szücs, J. Chenu, N. El Arbi, and F. Brouillard, J. Phys. B **29**, 2837 (1996).
[22] T. Nzeyimana, E. A. Naji, X. Urbain, and A. Le Padellec, Eur. Phys. J. D **19**, 315 (2002).
[23] E. Staicu-Casagrande, T. Nzeyimana, E. A. Naji, N. de Ruette, B. Fabre, A. Le Padellec, and X. Urbain, Eur. Phys. J. D **31**, 469 (2004).
[24] S. Srivastava, N. Sathyamurthy, and A. Varandas, Chem. Phys. **398**, 160 (2012).
[25] J. Loreau, J. Lecointre, X. Urbain, and N. Vaeck, Phys. Rev. A **84**, 053412 (2011).